Research Square

Preprints are preliminary reports that have not undergone peer review.
They should not be considered conclusive, used to inform clinical practice,
or referenced by the media as validated information.

Diagnostic Performance of Qualitative EBUS Elastography in Mediastinal Lymph Node Evaluation

mustafa erelel
Istanbul University
emine bensu erdemir
bensuerdemir@hotmail.com
Istanbul University
Ulku ardil
Istanbul University
Gudrat Badalov
Istanbul University
halim Issever
Istanbul University
mesude yasemin ozluk
Istanbul University
dogu bakkaloglu
Istanbul University
gorkem durak
Northwestern University

Research Article

Keywords: endobronchial ultrasound, elastography, mediastinal lymph nodes, lung cancer staging, qualitative elastography

Posted Date: August 31st, 2026

DOI: https://doi.org/10.21203/rs.3.rs-9917223/v1

License: This work is licensed under a Creative Commons Attribution 4.0 International License.
Read Full License

Additional Declarations: No competing interests reported.

Abstract

Background/Purpose:

Accurate assessment of mediastinal lymph node malignancy is essential for lung cancer staging. Current methods, such as positron emission tomography/computed tomography (PET-CT) or invasive sampling, have limitations and risks. Qualitative EBUS elastography (QEE) may offer an alternative for real-time assessment of nodal malignancy without requiring expensive quantitative tools or invasive procedures.

Methods

In this retrospective study, mediastinal and hilar lymph nodes were assessed using QEE features: Izumo stiffness score, intranodal color heterogeneity, and contour irregularity. Lymph node characteristics, PET-CT, and mediastinoscopy findings were recorded. Histopathology served as the reference standard. The diagnostic performance of QEE was evaluated using sensitivity, specificity, positive and negative predictive values, accuracy, and the area under the receiver operating characteristic curve.

Results

A total of 237 lymph nodes with definitive histopathological diagnoses were included. No malignant node (n = 98) showed an Izumo stiffness score-1 pattern. Malignant nodes more frequently showed score-3 stiffness than benign or granulomatous nodes (79/98 vs 12/107 vs 6/32, $p < 0.001$).Internal heterogeneity and contour irregularity were also significantly more common in malignant nodes (both $p < 0.001$). Using score 3 as the cutoff for malignancy, QEE achieved 80.6% sensitivity, 87.1% specificity, 81.4% positive predictive value, 86.4% negative predictive value, 84.4% accuracy, and an AUC of 0.818. PET-CT showed high sensitivity in malignant nodes (88/98, 89.8%) but also frequent false-positive findings in benign (40/107, 37.4%) and granulomatous nodes (25/32, 78.1%).

Conclusion

QEE has significant potential to improve the characterization of mediastinal lymph nodes and to inform biopsy decisions, particularly when PET-CT specificity is limited.

Key Findings

- No malignant lymph nodes demonstrated elastography score-1 stiffness, whereas score-3 stiffness was observed in 80.6% of malignant nodes (n = 79/98) (AUC: 0.81). This supports the potential value of QEE as a rule-out tool for malignancy while maintaining high accuracy in detecting true malignancy.

- In our cohort, the false-positive lymph node count was 65 on PET scans and 18 on QEE, indicating that QEE has the potential to improve false-positive PET cases.
- Among lymph nodes visualized by EBUS but not sampled by EBUS-TBNA due to technical or anatomical limitations and subsequently evaluated by mediastinoscopy, 45 of 55 score-3 lymph nodes were histopathologically malignant (81.8%).

Introduction

Nodal metastasis is one of the strongest predictors of survival in lung cancer. Five-year survival declines progressively with increasing nodal burden, from approximately 50–60% in N0 disease to 30–40% in N1 disease, around 15–25% in N2 disease, and the poorest outcomes in N3 disease [1, 3]. Even a single metastatic mediastinal node can upstage a potentially resectable tumor to stage III, eliminating surgical options and shifting management toward chemoradiotherapy or systemic treatment[2]. Because therapeutic decision-making and expected survival depend heavily on the presence and extent of nodal disease, precise characterization of mediastinal lymph nodes is essential for selecting the optimal treatment strategy and for avoiding unnecessary invasive procedures[4] .

Traditional imaging modalities, despite their central role in evaluating lung cancer, have well-known limitations. In the American College of Chest Physicians (ACCP) evidence-based guideline, the median sensitivity and specificity of computed tomography (CT) for detecting mediastinal lymph node metastasis were reported as 55% and 81%, respectively, indicating that CT may both miss malignant nodes and falsely classify benignly enlarged nodes as malignant [4, 5]. Although PET-CT is more accurate than CT for mediastinal staging, false-positive uptake may occur in inflammatory or granulomatous diseases such as tuberculosis and sarcoidosis, whereas false-negative results may occur in small-volume or microscopic nodal metastases. Therefore, PET-CT findings should not be used as the sole basis for mediastinal staging, and tissue confirmation is recommended when nodal involvement would alter treatment decisions [6, 7]. Additionally, these modalities rely solely on size- and metabolism-based criteria, leading to missed micrometastatic disease or false-positive findings in inflammatory and granulomatous conditions [5, 6]. Furthermore, inadequate use of Endobronchial Ultrasound-Guided Transbronchial Needle Aspiration (EBUS-TBNA) may lead to clinically significant staging errors, primarily due to incomplete sampling of mediastinal stations [3, 4]. These errors can result in inappropriate surgical referral, delayed definitive treatment, or unnecessary invasive procedures [3, 4].

In contrast, guideline-concordant, systematic EBUS-based staging algorithms can reduce the need for mediastinoscopy while maintaining high diagnostic accuracy and lowering procedure-related morbidity. To enhance diagnostic precision, elastography has been incorporated into modern EBUS systems, enabling real-time visualization of tissue elasticity through color-coded mapping. EBUS elastography enables real-time assessment of lymph node stiffness and has emerged as a promising adjunctive technique for differentiating benign from malignant mediastinal and hilar lymph nodes. Early clinical

studies demonstrated that elastographic color patterns may help distinguish malignant from benign lymph nodes during EBUS evaluation. More recent meta-analyses report high pooled diagnostic performance, with sensitivities and specificities approaching 93% and 85%, respectively. These findings support the use of EBUS elastography as a complementary tool to conventional EBUS-TBNA in thoracic nodal assessment [8–10].

Most previous studies have evaluated EBUS elastography using semi-quantitative or quantitative parameters, such as strain ratio, stiffness area ratio, or blue color ratio. Although these measurements may provide objective information, they can be technically variable and less practical in routine clinical settings. In contrast, qualitative elastographic assessment based on color distribution or stiffness patterns may offer a simpler, more clinically applicable approach to estimating malignancy risk in mediastinal and hilar lymph nodes [11–14]. The aim of this study was to retrospectively evaluate the diagnostic performance of QEE in differentiating benign, malignant, and granulomatous mediastinal and hilar lymph nodes, using histopathological outcome as the reference standard.

Materials and Methods

Study Design

This retrospective study was conducted at the Bronchoscopy Unit of Istanbul Faculty of Medicine from January 2023 to October 2025. All patients were managed according to routine clinical practice, and data were obtained from institutional electronic medical records. For each case, demographic, clinical, radiological (CT and PET-CT), and pathological data were collected. Recorded variables included PET-CT uptake status, short- and long-axis lymph node diameters, elastographic color pattern and stiffness score, and mediastinoscopy findings. Diagnostic concordance between EBUS-TBNA and mediastinoscopy was also assessed. Only cases with complete clinical, radiological, elastographic, and pathological data were included in the final analysis. Patient-level and lymph node-level data were reported separately to avoid ambiguity in the study flow.

Inclusion and Exclusion Criteria

A total of 279 patients who underwent EBUS-TBNA were initially enrolled. Patients were included if they presented with mediastinal or hilar lymphadenopathy (short-axis ≥ 10 mm) confirmed by thoracic imaging (CT, PET-CT, or both) and underwent elastography during EBUS-TBNA. Patients were excluded if elastography imaging was not performed during the EBUS procedure (for any reason), if a definitive histopathological diagnosis could not be established—since pathology served as the gold standard reference—or if clinical records were incomplete or biopsy material was insufficient. Cases with indeterminate pathology reports were also excluded from the study.

Of the 279 initially screened patients, 36 were excluded for insufficient clinical data, and 28 for inability to perform elastography during the EBUS procedure. The final cohort, therefore, included 215 patients.

Among these patients, 254 mediastinal or hilar lymph nodes were sampled; 237 yielded a definitive histopathological diagnosis and were included in the primary diagnostic performance analysis, whereas 17 were non-diagnostic and excluded from the performance calculations.

Qualitative EBUS Elastography Assessment

EBUS-TBNA was performed under conscious sedation with midazolam and topical 2% lidocaine anesthesia, using a convex-probe bronchoscope (Pentax EB19-J10U). Mediastinal and hilar lymph nodes were systematically evaluated in real time, and nodal stations were classified according to the International Association for the Study of Lung Cancer (IASLC) lymph node map.

QEE was used to assess nodal stiffness, producing real-time color maps in which red/green indicated softer tissue and blue indicated higher stiffness. Each lymph node was assigned a three-tier qualitative stiffness score according to the Izumo classification: score 1, predominantly non-blue/soft pattern; score 2, mixed blue and non-blue pattern; and score 3, predominantly blue/stiff pattern. Internal heterogeneity was defined as a non-uniform intranodal elastographic color pattern, and contour irregularity was defined as asymmetric, lobulated, or ill-defined nodal borders on elastographic imaging. No strain-ratio or quantitative elastography measurements were used. All elastographic recordings were digitally stored and reviewed by two experienced bronchoscopists with 30 and 5 years of interventional bronchoscopy experience. The final score was assigned by consensus.

Histopathological Evaluation

All EBUS-TBNA specimens were processed in accordance with institutional pathology protocols. Cytological smears and cell-block preparations were independently evaluated by two pulmonary pathologists with 10 years of experience, who were blinded to elastography findings. In selected cases, core tissue biopsies obtained during EBUS or subsequent mediastinoscopy were also reviewed to provide histological confirmation. Histopathological diagnosis served as the reference standard. For benign or granulomatous diagnoses based solely on EBUS-TBNA, diagnostic confirmation was supported by clinical and radiological follow-up.

Each case was assigned to one of three categories: benign, granulomatous, or malignant. The benign group included reactive and anthracotic lymphadenopathy without granulomatous or malignant features. The granulomatous group included lymph nodes with histologically confirmed granulomas, including non-necrotizing granulomas, as well as cases of tuberculosis, sarcoidosis, and other granulomatous inflammatory conditions. The malignant group included primary lung cancer, lymphoma, and metastatic disease from extrapulmonary primaries. Cases with bronchial epithelium, non-diagnostic samples, or insufficient material were excluded to ensure diagnostic accuracy.

Statistical Analysis

All statistical analyses were conducted using IBM SPSS Statistics (IBM Corp., Armonk, NY, USA). Continuous variables were reported as mean ± standard deviation (SD) or median (IQR), and categorical variables as counts and percentages. Comparisons among malignant, benign, and granulomatous lymph nodes were performed using chi-square or Fisher's exact tests for categorical variables and t-tests, one-way ANOVA, or nonparametric equivalents for continuous variables, as appropriate.

Associations among elastographic features, PET status, and histopathological diagnosis were evaluated using contingency table analyses. The diagnostic performance of QEE was assessed using an elastography score of 3 as the predefined threshold for malignancy. Sensitivity, specificity, positive predictive value, negative predictive value, overall diagnostic accuracy, and AUC were calculated for elastography and PET-CT. A separate subgroup analysis was performed on mediastinoscopy-confirmed lymph nodes visualized by EBUS but not sampled due to technical or anatomical limitations. A two-tailed p-value < 0.05 was considered statistically significant.

Results

The patient selection process and lymph node inclusion flow are shown in Fig. 1.

Patients with malignant disease were significantly older than those with benign or granulomatous disease, with mean ages of 64.1 ± 8.7, 59.8 ± 10.4, and 55.6 ± 11.2 years, respectively ($p < 0.001$). Male predominance was more frequent in the malignant group (86.5%) than in the benign and granulomatous groups (70.3% and 68.0%, respectively; $p = 0.02$). Smoking history was more common among patients with malignant disease (89.9%) compared with those with benign (62.4%) or granulomatous disease (60.0%) ($p < 0.05$). Similarly, mean cumulative smoking exposure was highest in the malignant group, followed by the benign and granulomatous groups: 41.2 ± 24.6, 28.5 ± 19.7, and 18.3 ± 14.1 pack-years, respectively. Baseline demographic and clinical characteristics according to diagnostic group are summarized in Table 1.

Table 1
Baseline demographic and clinical characteristics according to diagnostic group.

Variable	Malignant group (n = 89)	Benign group (n = 101)	Granulomatous group (n = 25)	p value
Age, years, mean ± SD	64.1 ± 8.7	59.8 ± 10.4	55.6 ± 11.2	< 0.001
Male sex, n (%)	77 (86.5%)	71 (70.3%)	17 (68.0%)	0.02
Smoking history, n (%)	80 (89.9%)	63 (62.4%)	15 (60.0%)	< 0.05
Smoking,pack-years, mean ± SD	41.2 ± 24.6	28.5 ± 19.7	18.3 ± 14.1	< 0.001
Known primary malignancy, n (%)	29 (32.6%)	16 (15.8%)	2 (8.0%)	0.01
Hypertension, n (%)	43 (48.3%)	41 (40.6%)	11 (44.0%)	0.58
Coronary artery disease, n (%)	18 (20.2%)	13 (12.9%)	3 (12.0%)	0.31
Diabetes mellitus, n (%)	21 (23.6%)	17 (16.8%)	6 (24.0%)	0.63
COPD, n (%)	20 (22.5%)	5 (5.0%)	1 (4.0%)	< 0.001
SD: standard deviation; COPD: chronic obstructive pulmonary disease.				

Among patients with a known primary malignancy, mediastinal lymph nodes were histopathologically malignant in 29 of 47 patients (61.7%), benign in 16 (34.0%), and granulomatous in 2 (4.3%). The most common primary malignancy was lung cancer, followed by breast cancer, colorectal cancer, and lymphoma.

Overall, among 237 lymph nodes, 98 (41.4%) were malignant, 107 (45.1%) were benign, and 32 (13.5%) were granulomatous (Table 2). The most frequently sampled nodal stations were the subcarinal station (station 7), right lower paratracheal station (4R), and left lower paratracheal station (4L), representing 121 (47.6%), 78 (30.7%), and 17 (6.7%) of all sampled nodes, respectively. Mean short-axis and long-axis diameters were 16.7 ± 7.5 mm and 20.8 ± 9.7 mm in malignant lymph nodes, 17.5 ± 4.7 mm and 19.4 ± 9.3 mm in granulomatous lymph nodes, and 13.3 ± 5.4 mm and 18.9 ± 9.0 mm in benign lymph nodes, respectively ($p < 0.05$).

Table 2
Subtype Distribution of Lymph Nodes

Category	Subtype	Number (n)	Percentage (%)
Malignant (n = 98)	Squamous cell carcinoma	36	36.7
	Adenocarcinoma	23	23.5
	Small-cell carcinoma	20	20.4
	Other malignancies	19	19.4
Benign (n = 107)	Reactive lymphoid hyperplasia	50	46.7
	Others	57	53.3
Granulomatous (n = 32)	Non-necrotizing granulomas	16	50.0
	Tuberculosis	7	21.9
	Sarcoidosis	5	15.6
	Other granulomatous inflammation	4	12.5

Among malignant nodes (n = 98), the most common subtypes were squamous cell carcinoma (36.7%), adenocarcinoma (23.5%), and small-cell carcinoma (20.4%). Benign nodes (n = 107) were predominantly reactive or nonspecific, with reactive lymphoid hyperplasia alone accounting for 46.7%. Granulomatous nodes (n = 32) consisted primarily of non-necrotizing granulomas, with the remainder diagnosed as tuberculosis (21.9%) or sarcoidosis (15.6%). The distribution of lymph-node pathological subtypes is presented in Table 2.

Benign nodes predominantly showed intermediate stiffness, with 71% (76/107) assigned a score of 2 and 11% (12/107) a score of 3. Granulomatous nodes showed a similar pattern (score 2: 75% [24/32]; score 3: 19% [6/32]). In contrast, malignant nodes exhibited markedly increased stiffness, with 81% (79/98) scoring 3 and 19.4% (19/98) scoring 2; notably, no malignant node received a score of 1 (global chi-square $p = 1.06 \times 10^{-23}$; $p < 0.001$ for malignant vs. non-malignant). Internal heterogeneity ($p < 0.001$) and contour irregularity ($p < 0.001$) also showed significant diagnostic separation, with each feature showing progressively higher abnormality among malignant nodes. The distribution of elastography stiffness scores and morphologic elastographic features across pathology groups is shown in Table 3. Representative elastographic patterns are illustrated in Fig. 2.

Table 3
Distribution of elastography stiffness scores and morphologic features across pathology groups. No malignant node demonstrated a score of 1 ($\chi^2 = 113.91$; df = 4; $p < 0.001$).

Pathology \ Score	Score 1 (n/%)	Score 2 (n/%)	Score 3 (n/%)	Heterogeneity (n/%)	Irregular Contour (n/%)	Total
Malignant (n = 98)	0 (0%)	19 (19.4%)	79 (80.6%)	59 (60.2%)	66 (67.3%)	98
Benign (n = 107)	19 (17.8%)	76 (71%)	12 (11.2%)	12 (11.2%)	18 (16.8%)	107
Granulomatous (n = 32)	2 (6.3%)	24 (75%)	6 (18.8%)	7 (21.9%)	7 (21.9%)	32
Total	21	119	97	78 (32.9%)	91 (38.4%)	237

χ^2: chi-square; df: degrees of freedom.

Morphologic elastographic features were also evaluated: malignant nodes showed significantly greater internal heterogeneity (60.2%) and contour irregularity (67.3%) than benign nodes (11.2% and 16.8%, respectively) (both $p < 0.001$). Granulomatous nodes showed intermediate disruption (21.9% and 21.9%).

PET-CT integrated analysis showed PET positivity in 89.8% of malignant lymph nodes (88/98), 37.4% of benign nodes (40/107), and 78.1% of granulomatous nodes (25/32). Based on the presented confusion matrix, PET-CT had a sensitivity of 89.8%, specificity of 53.2%, positive predictive value (PPV) of 57.5%, negative predictive value (NPV) of 88.1%, and overall accuracy of 68.4%. The PET-CT confusion matrix is presented in Table 4. In contrast, elastography score-3 stiffness was observed in 80.6% of malignant nodes (79/98), compared with 11.2% of benign nodes (12/107) and 18.8% of granulomatous nodes (6/32) ($p < 0.001$). The elastography confusion matrix is shown in Table 5.

Table 4
Confusion Matrix of PET-CT

PET Positive	Histopathologically Malignant	Histopathologically Non-Malignant	Total
	88 (True Positive)	**65 (False Positive)**	**153**
PET Negative	10 (False Negative)	74 (True Negative)	84
Total	98	139	237

PET-CT: positron emission tomography-computed tomography.

Table 5
Confusion Matrix of Qualitative EBUS Elastography (Score 3 = Positive for Malignancy)

Elastography Positive (Score 3)	**Histopathologically Malignant**	**Histopathologically Non-Malignant**	**Total**
	79 (True Positive)	**18 (False Positive)**	**97**
Elastography Negative (Score 1–2)	19 (False Negative)	121 (True Negative)	140
Total	98	139	237

EBUS: endobronchial ultrasound.

In an exploratory mediastinoscopy-confirmed subset, 55 lymph nodes that were visualized by EBUS but not sampled by EBUS-TBNA because of anatomical or technical limitations showed score-3 stiffness on elastography. Among these, 45 lymph nodes were histopathologically malignant (81.8%), whereas 10 were non-malignant (18.2%). Because this subset included only score-3 lymph nodes, no diagnostic performance comparison or p-value was calculated.

Using an elastography score of 3 as the predefined threshold for malignancy, QEE achieved a sensitivity of 80.6% (95% confidence interval [CI]: 71.4–87.6), specificity of 87.1% (95% CI: 79.8–92.3), positive predictive value of 81.4% (95% CI: 72.3–88.0), negative predictive value of 86.4% (95% CI: 79.0–91.7), and overall diagnostic accuracy of 84.4% (95% CI: 78.9–88.8), with an area under the curve (AUC) of 0.818 (95% CI: 0.764–0.872) ($p < 0.001$).

Discussion

This single-center retrospective study evaluated the diagnostic value of QEE for assessing mediastinal and hilar lymph nodes. The main finding was that an elastography score of 3 was strongly associated with malignancy, whereas no malignant lymph node had a score of 1. In addition, malignant nodes exhibited significantly greater internal heterogeneity and contour irregularity than benign and granulomatous nodes.

Our study has several notable strengths, including a relatively large lymph node cohort with histopathological correlation, inclusion of benign, malignant, and granulomatous lymphadenopathy, and evaluation of a clinically practical qualitative elastography approach that can be readily integrated into routine EBUS workflows. Unlike quantitative elastography techniques, which often require dedicated software, incur additional costs, involve region-of-interest selection, and require post-processing analysis, QEE can be performed in real time during bronchoscopy without additional equipment or added workflow complexity. This makes it particularly feasible and practical for routine clinical practice and for centers where advanced quantitative analysis may not be readily available. The AUC of 0.818 observed in our study supports the effectiveness of this simpler, real-time approach, though its observer-dependent nature should be acknowledged.

From a clinical perspective, the greatest value of QEE may lie not in replacing tissue diagnosis but in improving procedural decision-making during mediastinal staging. In patients with multiple enlarged lymph nodes, elastography may help identify the most suspicious targets for sampling, prioritize biopsy order, guide allocation of needle passes, and increase operator confidence when conventional imaging findings are equivocal. This may be particularly relevant in regions with a high prevalence of granulomatous disease, where PET-CT specificity is often lower. An additional finding of our study was the lower false-positive rate of QEE compared with PET-CT. This observation may be particularly relevant in granulomatous diseases, where increased metabolic activity frequently results in PET positivity despite the absence of malignancy. In our cohort, QEE demonstrated higher specificity than PET-CT in this setting, suggesting that it may serve as a reliable adjunctive tool for the evaluation of PET-positive mediastinal lymph nodes. However, this increased specificity was accompanied by a modest reduction in sensitivity, indicating that some malignant lymph nodes may not exhibit a score-3 elastographic pattern. Therefore, QEE should be considered complementary to, rather than a replacement for, established staging modalities and histopathological confirmation.Our results are consistent with earlier studies showing that malignant lymph nodes tend to be stiffer on EBUS elastography and with its potential to differentiate benign from malignant intrathoracic lymph nodes [15–17]. Chen et al. reported pooled sensitivities and specificities of approximately 0.93 and 0.85, respectively, suggesting that tissue stiffness is a reproducible marker of malignant nodal involvement across different patient populations and elastography techniques [9]. The diagnostic performance observed in our cohort supports this concept and indicates that the biological alterations associated with malignant infiltration can also be captured through qualitative elastographic assessment without the need for complex quantitative measurements.

The mediastinoscopy-confirmed subgroup provides an additional observation: among lymph nodes visualized by EBUS but not sampled because of anatomical or technical limitations, score-3 stiffness was frequently associated with malignancy. This finding suggests that elastography may provide useful information even when direct EBUS-TBNA sampling is not feasible. However, this subgroup should be interpreted cautiously because it was selected based on technical and anatomical considerations rather than systematic sampling criteria. Therefore, these results should be considered hypothesis-generating and require validation in prospective studies with predefined inclusion criteria and standardized correlation with mediastinoscopy.

Nevertheless, QEE should not be regarded as a substitute for histopathological confirmation. Current mediastinal staging strategies emphasize tissue diagnosis when nodal status will influence treatment decisions, and EBUS-TBNA remains a central minimally invasive method for pathological confirmation.

Limitations

This study has several limitations. First, its retrospective, single-center design may introduce selection bias and limit the generalizability of the findings. Second, the analysis was performed at the lymph node level, and some patients contributed more than one lymph node; therefore, clustering within patients

may have influenced the statistical estimates. Third, quantitative elastography measurements, such as strain ratio, stiffness area ratio, or blue color ratio, were not obtained since they requires additional software, precluding direct comparison between qualitative and quantitative elastographic methods. Fourth, elastographic features were evaluated by consensus rather than by independent observers; therefore, interobserver agreement could not be assessed. Future studies should include independent readers and report kappa statistics for stiffness score, internal heterogeneity, and contour irregularity. Fifth, although benign and granulomatous diagnoses were supported by clinical and radiological follow-up, surgical confirmation was available only in a subset of patients. Finally, the mediastinoscopy-confirmed subset was selected because technical or anatomical limitations during EBUS-TBNA may limit the generalizability of this subgroup analysis to the broader study population. Moreover, this subset included only lymph nodes with score-3 stiffness; therefore, it could not be used to calculate diagnostic performance or compare elastography score categories.

Conclusions

In conclusion, QEE demonstrated promising diagnostic performance in differentiating malignant from non-malignant mediastinal and hilar lymph nodes. Stiffness score 3, internal heterogeneity, and contour irregularity were significantly associated with malignancy. Importantly, no malignant lymph nodes had a stiffness score of 1, indicating that QEE has the potential to be a robust rule-out tool for malignancy. Our study showed that QEE offers higher specificity than PET-CT, particularly for granulomatous lymph nodes, at the expense of lower sensitivity. These findings support its use as a practical, real-time adjunct to EBUS-TBNA and PET-CT, while reinforcing that final clinical decisions should continue to rely on histopathological confirmation.

Declarations

Funding

No financial support was received for this study.

Clinical trial number

not applicable.

Consent for Publication

Not applicable.

Availability of Data and Materials

The datasets generated and/or analyzed during the current study are not publicly available due to institutional and patient confidentiality regulations but are available from the corresponding author on reasonable request.

Acknowledgements

Not applicable.

Conflict of Interest

The authors declare no conflict of interest.

This study was approved by the Clinical Research Ethics Committee of Istanbul Faculty of Medicine, Istanbul University (Approval No: 2025/1381; Meeting No: 18; Date: 05 September 2025). The study titled “Diagnostic Value of Elastography for Differentiating Malignant and Benign Mediastinal Lymph Nodes” was conducted under the supervision of Prof. Dr. Mustafa Erelel, Department of Pulmonology, Istanbul Faculty of Medicine. The official ethics approval letter was issued on 10 September 2025 (File No: E-29624016-050.99-3577369), and the final decision form on 11 September 2025 (File No: 2025-3577362). Given the retrospective nature of the study, the requirement for informed consent was waived. The research complied with the ethical principles set out in the Declaration of Helsinki.

Authors’ contributions

M.E. conceived and supervised the study, contributed to study design, clinical interpretation, and critical revision of the manuscript. E.B.E. collected the data, reviewed elastography findings, performed the statistical analyses, conducted the literature review, and drafted the manuscript. U.A. and G.B. contributed to patient evaluation, EBUS procedures, and clinical data acquisition. H.I. contributed to the statistical methodology and interpretation of the analyses. M.Y.O. and D.V.B. performed histopathological evaluations and contributed to pathological interpretation. G.D. contributed to radiological and elastographic interpretation and provided methodological guidance for imaging analysis. All authors reviewed, revised, and approved the final manuscript.

Ethical statements

This study was approved by the Clinical Research Ethics Committee of Istanbul Faculty of Medicine, Istanbul University (Approval No: 2025/1381; Meeting No: 18; Date: 05 September 2025). The official ethics approval letter was issued on 10 September 2025 (File No: E-29624016-050.99-3577369), and the final decision form on 11 September 2025 (File No: 2025-3577362). Given the retrospective nature of the study, the requirement for informed consent was waived. The study was conducted in accordance with the ethical principles of the Declaration of Helsinki.

References

1. Rusch VW, Crowley J, Giroux DJ, et al. The IASLC Lung Cancer Staging Project: proposals for the revision of the N descriptors in the forthcoming seventh edition of the TNM classification for lung cancer. J Thorac Oncol. 2007;2:603–12. 10.1097/JTO.0b013e31807ec803.

2. Flury DV, Jaksic S, Caviezel C, et al. Heterogeneity of stage IIIA non-small cell lung cancer—different surgical strategies. Curr Chall Thorac Surg. 2022;4:14. 10.21037/ccts-21-43.
3. Herth FJF, Krasnik M, Kahn N, et al. Combined endobronchial and esophageal endosonography for the diagnosis and staging of lung cancer. Eur Respir J. 2010;35:295–300.
4. Silvestri GA, Gonzalez AV, Jantz MA, et al. Methods for staging non-small cell lung cancer: diagnosis and management of lung cancer, 3rd ed: American College of Chest Physicians evidence-based clinical practice guidelines. Chest. 2013;143:eS211–50. 10.1378/chest.12-2355.
5. Xia Y, Zhang B, Zhang H, et al. Evaluation of lymph node metastasis in lung cancer: who is the chief justice? J Thorac Dis. 2015;7:S231–7. 10.3978/j.issn.2072-1439.2015.11.63.
6. Gould MK, Kuschner WG, Rydzak CE, et al. Test performance of positron emission tomography and computed tomography for mediastinal staging in patients with non-small-cell lung cancer: a meta-analysis. Ann Intern Med. 2003;139:879–92. 10.7326/0003-4819-139-11-200311180-00013.
7. Werutsky G, Hochhegger B, Figueiredo Pinto JAL, et al. PET-CT has low specificity for mediastinal staging of non-small-cell lung cancer in an endemic area for tuberculosis: a diagnostic test study. BMC Cancer. 2019;19:5. 10.1186/s12885-018-5233-5.
8. Izumo T, Sasada S, Chavez C, et al. Endobronchial ultrasound elastography in the diagnosis of mediastinal and hilar lymph nodes. Jpn J Clin Oncol. 2014;44:956–62. 10.1093/jjco/hyu105.
9. Chen YF, Mao XW, Zhang YJ, et al. Endobronchial ultrasound elastography differentiates intrathoracic lymph nodes: a meta-analysis. Ann Thorac Surg. 2018;106:1251–7. 10.1016/j.athoracsur.2018.04.086.
10. Wu J, Zhao Y, Wang J, et al. Diagnostic value of endobronchial ultrasound elastography for differentiating benign and malignant hilar and mediastinal lymph nodes: a systematic review and meta-analysis. Med Ultrason. 2022;24:85–94. 10.11152/mu-3173.
11. Zhang M, Li X, Chen H, et al. Diagnostic performance of endobronchial ultrasound elastography for mediastinal and hilar lymph nodes: an updated meta-analysis. Front Oncol. 2023;13:1195021.
12. Huang H, Huang Z, Wang Q, et al. Effectiveness of the benign and malignant diagnosis of mediastinal and hilar lymph nodes by endobronchial ultrasound elastography. J Cancer. 2017;8:1843–8. 10.7150/jca.19819.
13. Ma H, An Z, Xia P, et al. Semi-quantitative analysis of EBUS elastography as a feasible approach in diagnosing mediastinal and hilar lymph nodes of lung cancer patients. Sci Rep. 2018;8:3571. 10.1038/s41598-018-22006-4.
14. Mittal S, Mohan A, Hadda V, et al. Endobronchial ultrasound elastography in mediastinal lymphadenopathy: report of two cases and systematic review of literature. Lung India. 2019;36:149–53. 10.4103/lungindia.lungindia_349_17.
15. Rozman A, Malovrh MM, Adamic K, et al. Endobronchial ultrasound elastography strain ratio for mediastinal lymph node diagnosis. Radiol Oncol. 2015;49:334–40. 10.1515/raon-2015-0020.
16. Gu Y, Shi H, Su C, et al. The role of endobronchial ultrasound elastography in the diagnosis of mediastinal and hilar lymph nodes. Oncotarget. 2017;8:89194–202. 10.18632/oncotarget.19194.

17. Wang Y, Zhao Z, Zhu M, et al. Diagnostic value of endobronchial ultrasound elastography in differentiating between benign and malignant hilar and mediastinal lymph nodes: a retrospective study. Quant Imaging Med Surg. 2023;13:4648–62. 10.21037/qims-23-241.

Figures

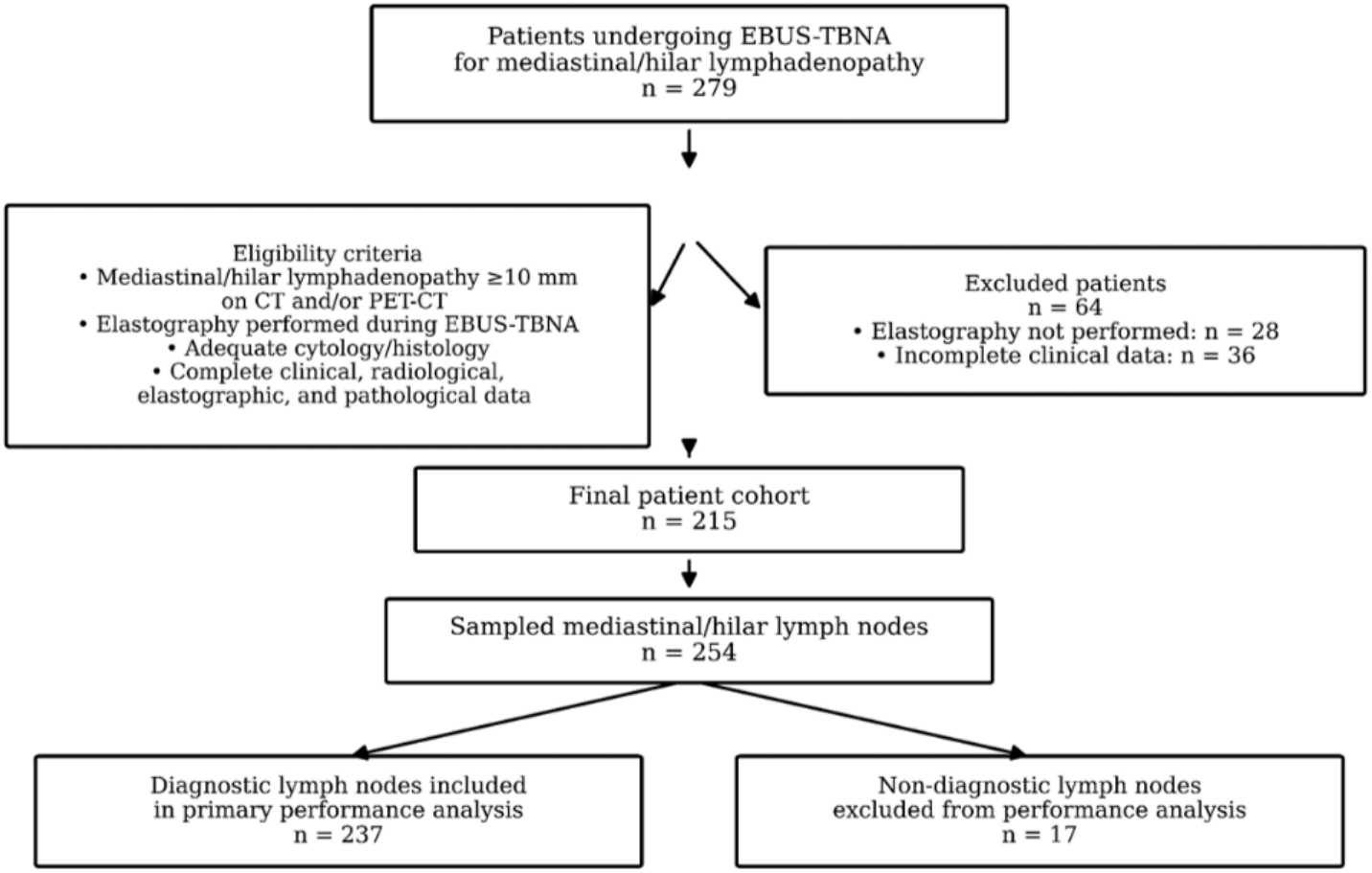
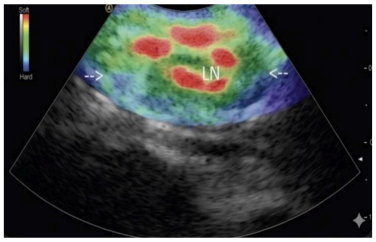


Figure 1

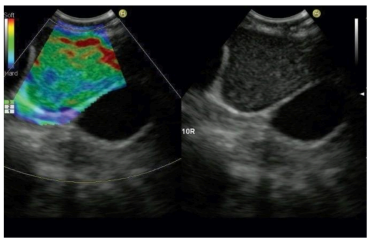
Flowchart of patient and lymph-node selection.

- **Figure 2. Representative elastographic patterns of mediastinal lymph nodes.**



- **(a) Normal lymph node EBUS image.**

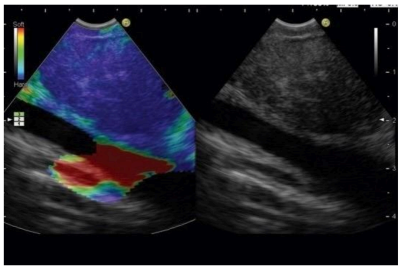
EBUS: endobronchial ultrasound.



- **(b) Score 1: Predominantly green, soft, and homogeneous elastographic appearance, indicating low stiffness.**



- **(c) Score 2: Mixed green-blue color distribution representing intermediate stiffness with partially preserved internal architecture.**



- **(d) Score 3: Predominantly blue, high-stiffness pattern, often accompanied by heterogeneity and contour irregularity; this pattern was associated with malignant involvement in the present cohort.**

Figure 2

See image above for figure legend